Supporting Information

Ziqi Ma,[a] Yin Liu,[a] Xue Li,[a] Xinqi Xu,[b] Rui Shi,[a] Shengli Zhu,[a, c] Zhenduo Cui,*[a] Zhaoyang Li,[a] Wence Xu,[a] Zhonghui Gao,[a] Jiamin Zhu,[a] Yanqin Liang,*[a] and Hui Jiang*[a, c]

1. Experimental section

Materials. The p-terphenyl (PT, 98%), 2,5-Bis(4-biphenylyl)thiophene (BP1T, 98%) and Polydimethylsiloxane (PDMS) was purchased from Tianjin Heowns Biochem Technologies Co. Ltd. The 5,5'-Di([1,1'-biphenyl]-4-yl)-2,2'-bithiophene (BP2T, 98%) and 2,5-bis[5-(4-phenylphenyl)thiophen-2-yl]thiophene (BP3T, 98%) was purchased from Zhengzhou Chemical Engineering Co. Ltd.

Characterizations. We used the Thermo Scientific Nicolet iS10 FTIR spectrometer to measure the infrared (IR) spectra in the range of 500-4000 cm^{-1}. The DX-2700BH diffractometer equipped with Cu Kα radiation (λ = 1.54056 Å) was used to measure X-ray diffraction patterns over a 2θ range of 5–50°. The experiment was conducted with a scan step of 0.02° and a step time of 0.2 s with a single silicon wafer as the substrate. The Raman spectroscopy measurements were performed using a DXR2xi Raman spectrometer (Thermo Fisher Scientific, USA). The spectral data were acquired across a wavenumber range of 200–3000 cm^{-1}. The UV-Vis absorption spectra were recorded on a Shimadzu UV-2700 spectrophotometer over 200–800 nm, using barium sulfate as the reference. The steady-state photoluminescence (PL) spectra of the crystals were acquired with an Edinburgh Instruments FLS1000 spectrophotometer. The fluorescence decay profiles were measured using the same instrument, employing a 375 nm laser as the excitation source. Radioluminescence analysis was conducted using a commercial miniature X-ray source coupled with an Edinburgh Instruments FS5 fluorescence spectrophotometer. X-ray images were acquired with a Canon EOS 700D camera connected to a tungsten-target X-ray tube (Moxtek).

2. Figures and Tables

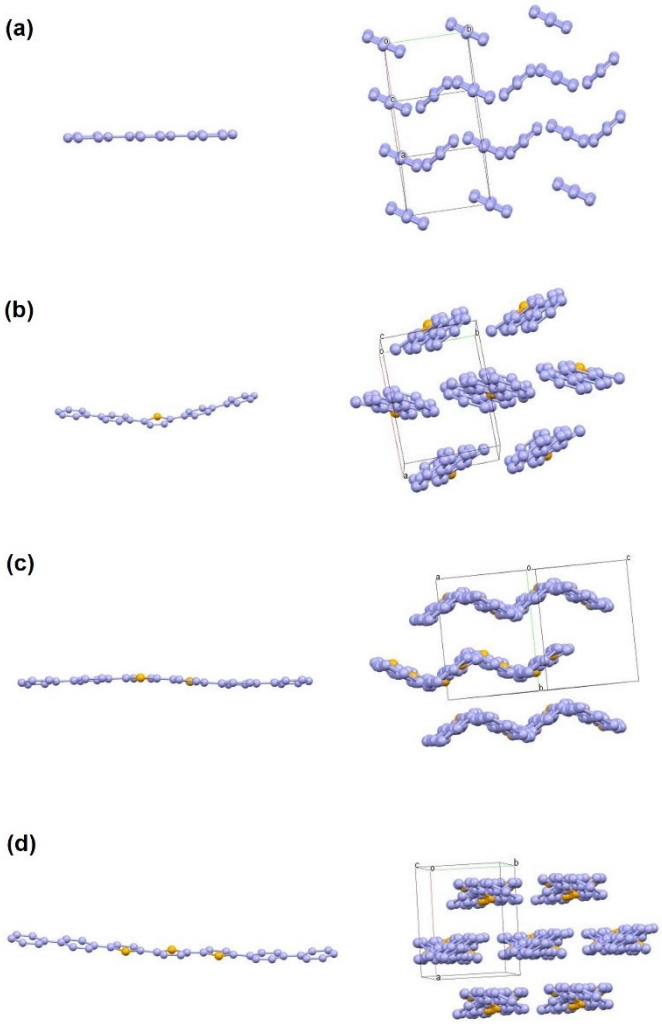

Figure S1. a). PT, b). BP1T, c). BP2T, d). BP3T molecular formula and crystal packing structure.

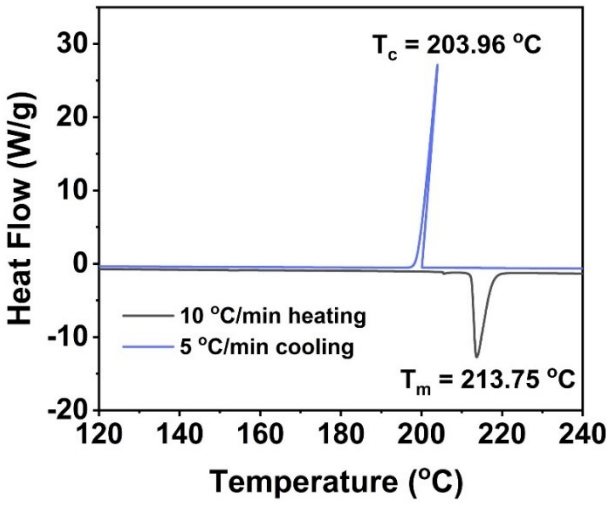

Figure S2. DSC results of PT single crystal.

Figure S3. PT single crystal before optimization under ultraviolet light.

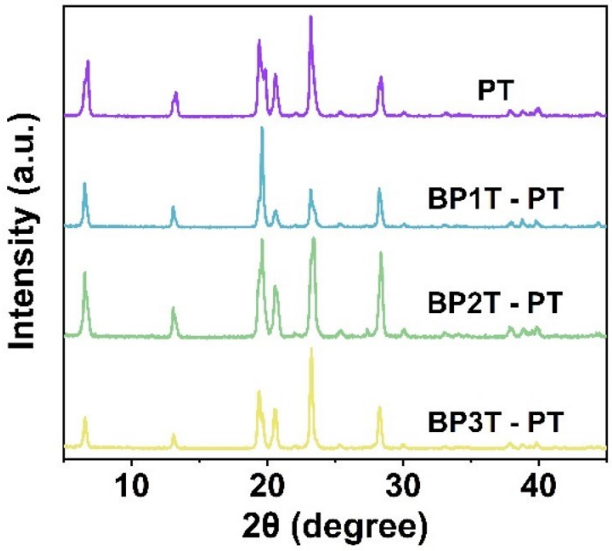

Figure S4. Powder X-ray diffraction patterns of PT, BP1T-PT, BP2T-PT, and BP3T-PT.

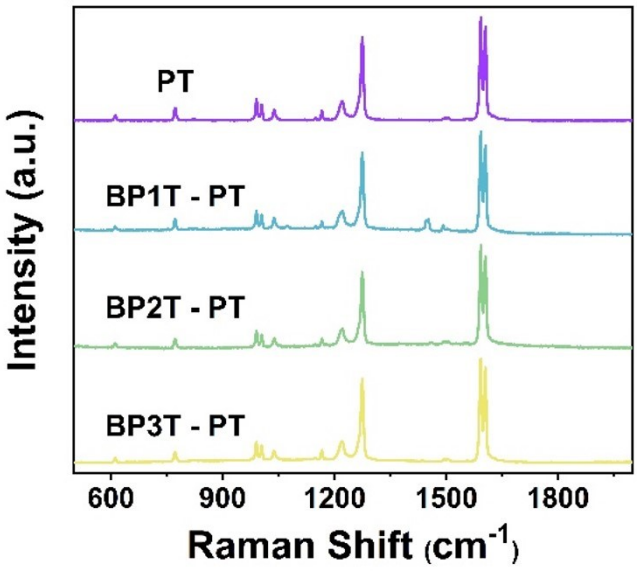

Figure S5. Raman patterns of PT, BP1T-PT, BP2T-PT, and BP3T-PT.

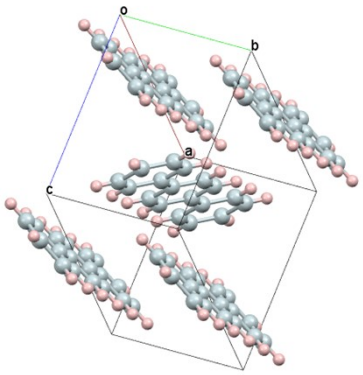

Figure S6. Crystal packing mode of BP1T-PT.

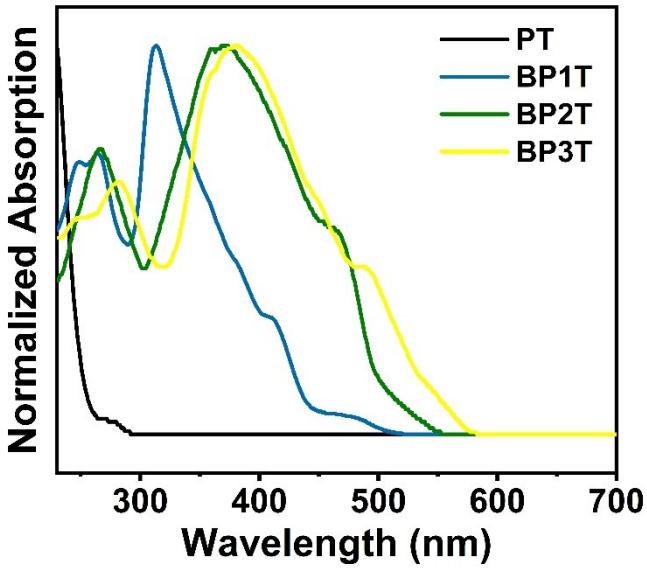

Figure S7. Ultraviolet-visible (UV-Vis) absorption spectra of PT, BP1T, BP2T, and BP3T.

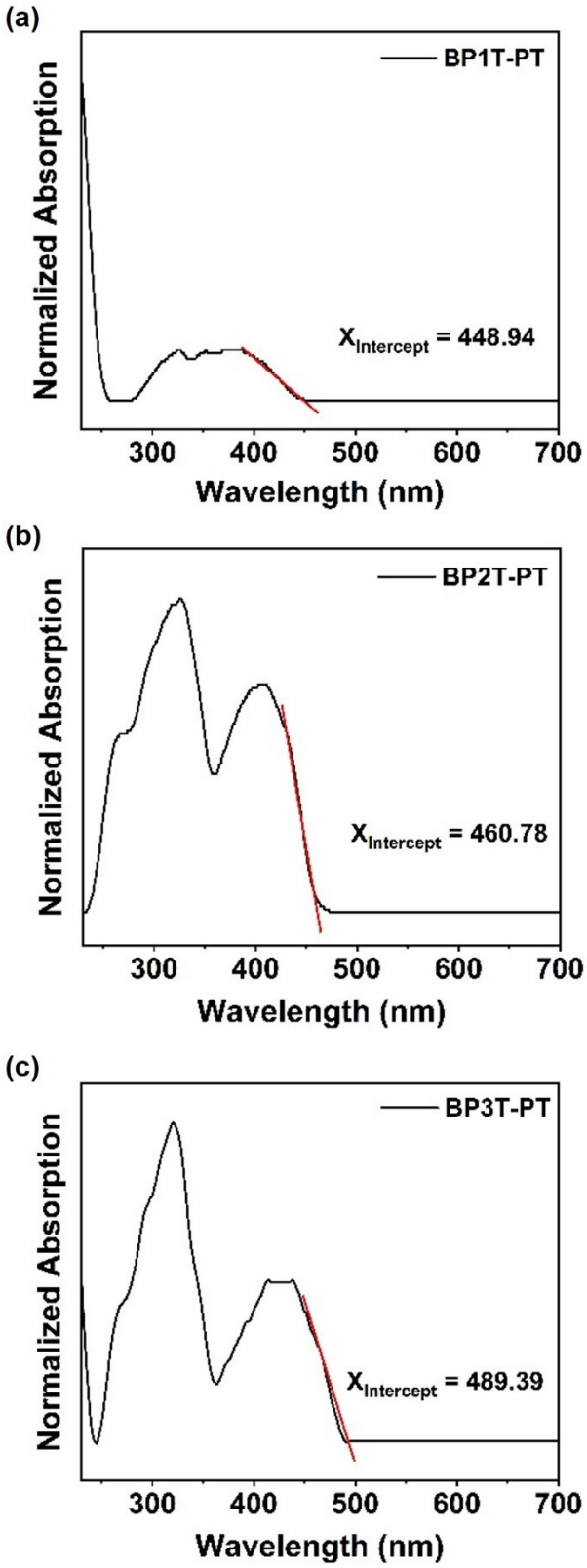

Figure S8. Solid-state UV–vis absorption spectra of a). BP1T-PT, b). BP2T-PT and c). BP3T-PT. And extrapolation of band gaps (red line).

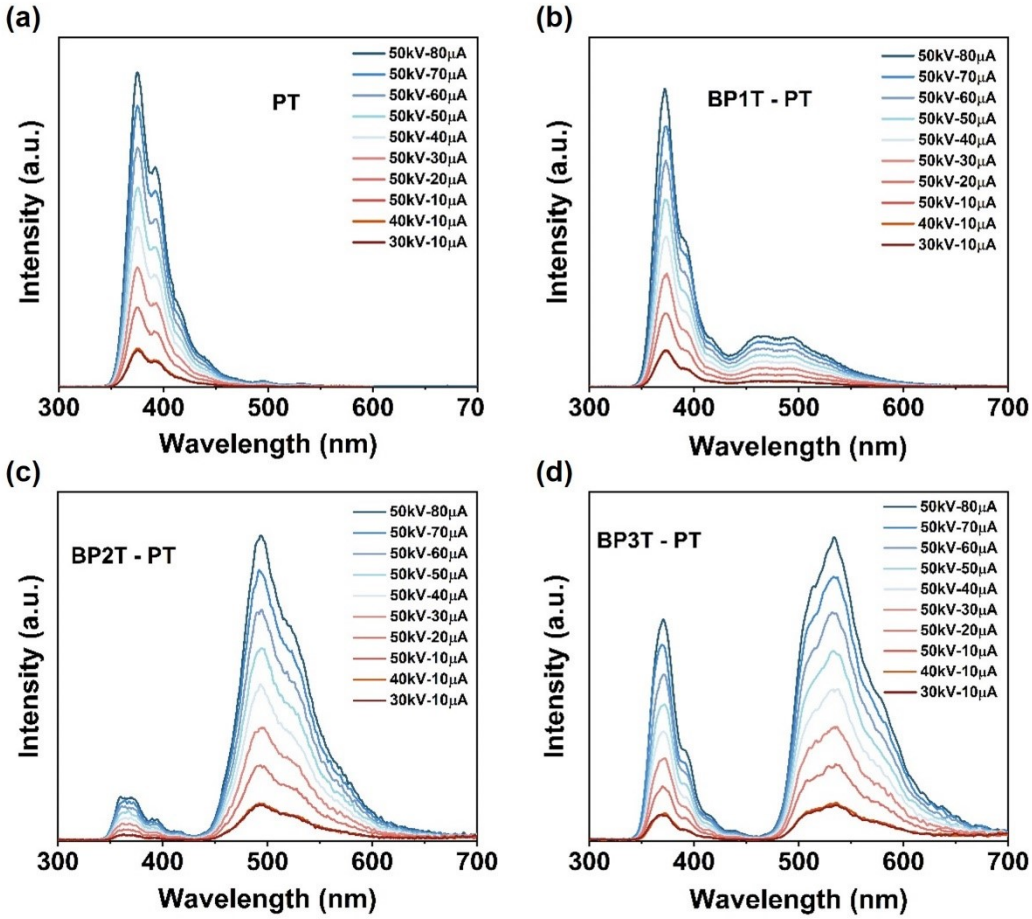

Figure S9. The dosage-dependent emission intensity in the range of 9.64 to 278 μGy/s of a). PT, b). BP1T-PT, c). BP2T-PT and d). BP3T-PT.

Table S1. Crystal structure data of BP1T-PT.

Crystal data	
Empirical formula	$C_{18}H_{14}$
Formula weight	230.29
Temperature/K	300.48(10)
Crystal system	monoclinic
Space group	$P2_1/c$
a, b, c (Å)	13.6141(4), 5.6164(2), 8.1130(3)
α, β, γ/°	90, 92.017(3), 90
Volume/Å^3	619.95(4)
Z	2
ρ_{calc}g/cm^3	1.234
μ/mm^{-1}	0.525
F(000)	244.0
Crystal size/mm^3	0.23 × 0.17 × 0.14
Radiation	Cu Kα (λ = 1.54184)
2Θ range for data collection/°	6.496 to 150.444
Index ranges	$-17 \le h \le 13$, $-6 \le k \le 6$, $-10 \le l \le 9$
Reflections collected	3391
Independent reflections	1209 [Rint = 0.0155, Rsigma = 0.0146]
Data/restraints/parameters	1209/0/82
Goodness-of-fit on F2	1.120
Final R indexes [I>=2σ (I)]	R1 = 0.0592, wR2 = 0.1783
Final R indexes [all data]	R1 = 0.0685, wR2 = 0.1877
Largest diff. peak/hole / e Å-3	0.20/-0.21

Table S2. Performance comparison of scintillators for X-ray imaging in the literature.

	Materials	Decay time (ns)	Reference
Our work	PT	2.24	
	BP1T-PT	0.3	
	BP2T-PT	0.44	
	BP3T-PT	0.5	
Other works	Anthracene	30	[1]
	Carbazole	11.4	[2]
	trans-Stilbene	4.5	[2]
	BIC	2.71	[3]
	p-Quaterphenyl	9.5	[2]
	CsI: Tl	1000	[4]
	CsPbBr3	200	[5]
	LaBr3:Ce	16	[6]
	TTM-1CzBr	18	[7]

3. Reference

1. A. Yamaji, S. Kurosawa, Y. Ohashi, Y. Yokota, K. Kamada and A. Yoshikawa, *Plasma and Fusion Research*, 2018, **13**, 2405011-2405011.
2. R. H. Ramprasath, M. S. Kajamuhideen, B. Tiwari and K. Sethuraman, *Journal of Materials Science: Materials in Electronics*, 2023, **34**, 620–631.
3. Q. Sun, H. Wang, J. Li, F. Li, W. Zhu, X. Zhang, Q. Chen, H. Yang and W. Hu, *Small Structures*, 2023, **4**, 2200275.
4. I. Mouhti, A. Elanique, M. Y. Messous, A. Benahmed, J. E. McFee, Y. Elgoub and P. Griffith, *Applied Radiation and Isotopes*, 2019, **154**, 108878.
5. J. H. Heo, D. H. Shin, J. K. Park, D. H. Kim, S. J. Lee and S. H. Im, *Advanced Materials*, 2018, **30**, 1801743.
6. S. Guo, K. Liu, Z. Lin, Z. Kang, J. Liu, Z. Yin, Z. Cai, Y. Liu, X. Zhang, F. Luo, S. Xiong, S. Wang, X. He, A. Yue, Q. Zhao, R. Guo and T. Wang, *Journal of Luminescence*, 2025, **277**, 120956.
7. A. Luo, J. Zhang, D. Xiao, G. Xie, X. Xu, Q. Zhao, C. Sun, Y. Li, Z. Zhang, P. Li, S. Luo, X. Xie, Q. Peng, H. Li, R. Chen, Q. Chen, Y. Tao and W. Huang, *Nature Communications*, 2024, **15**, 8181.